Australian Journal of Crop Science AJCS
AJCS 6(1):101-108 (2012) ISSN:1835-2707

Detection and mapping of hail damage to corn using domestic remotely sensed data in China

J. L. Zhao[1, 2], D. Y. Zhang[1], J. H. Luo[1], S. L. Huang[3], Y. Y. Dong[1], and W. J. Huang*[1]

[1]Beijing Research Center for Information Technology in Agriculture, Beijing Academy of Agriculture and Forestry Sciences, Beijing, P.R. China
[2]Institute of Remote Sensing Applications, Chinese Academy of Sciences, Beijing, P.R. China
[3]Key Laboratory of Intelligent Computing & Signal Processing, Ministry of Education, Anhui University, P.R. China

***Corresponding author: yellowstar0618@163.com**

Abstract

The objective of this study was to assess the hail damage to corn that occurred on July 14, 2010 in Gannan County, Qiqihar City, China, using two Huan Jing (HJ)-1-B (pre-hailstorm) and HJ-1-A (post-hailstorm) charge-coupled device (CCD) images of China. According to the change characteristics of normalised difference vegetation index (NDVI) of thirty field sampling points of post-hailstorm, a third-order polynomial was built between the NDIV difference (ΔNDVI) and Band 4 of the HJ-1-A CCD image. As a result, the coefficient of determination (R^2) of this model reached 91.62%; twenty sampling points were used to validate the model and R^2 reached 96.31%. Consequently, 8,575 ha of affected corn were monitored and the seriously affected corn area was 2,302.47 ha. Furthermore, the damage levels (light, moderate and serious) were also specified, the accuracy of which was validated by constructing a confusion matrix based on fifty ground truth points. The overall accuracy and Kappa coefficient (κ) were 86% and 0.7826, respectively. The results show that the degree of severity of injured corn gradually descended from the center to the margins, and the potential yield loss reached about 10,840 tons estimated by the serious damage level. This study suggests that multi-temporal and multispectral imagery of broadband HJ-1 CCD images of China are sufficient to assess hail-damaged areas and specify relative damage levels in corn.

Keywords: Change detection, Corn, Hail damage levels, HJ-1/CCD, NDVI, Remote sensing.
Abbreviations: ASD - Analytical spectral devices; CCD - Charge-coupled device; Chl - Chlorophyll content; CRESDA - China Centre for Resources and Satellite Data and Applications; ΔNDVI - NDVI difference; ENVI - Environment for visualising images; ETM+ - Enhanced thematic mapper plus; FLAASH - Fast line-of-sight atmospheric analysis of spectral hypercubes; GPS - Global Positioning System; HJ - Huan jing; κ - Kappa coefficient; LAI - Leaf area index; MODIS - Moderate resolution imaging spectroradiometer; NDVI - Normalised difference vegetation index; NIR - Near infrared; R^2 - Coefficient of determination, TM - Thematic mapper.

Introduction

Corn is an important crop in many places around the world; however, various limiting factors, especially with severe global climate change, have greatly caused production losses and quality reduction (Mirza 2003; Tai et al., 2011). Among those stress factors, extreme weather and climate events have imposed great negative effects on this crop. As meteorological disasters, hailstorms are also caused by abnormal climate change and have led to millions of dollars' worth of damage to crops (Golden et al., 1991). This weather condition is spatially random and varies greatly in intensity from hardly noticeable to catastrophic (Peters et al., 2000). Furthermore, crop hail damage is a major problem in the Great Plains, causing substantial losses in agriculture (Bentley et al., 2002). For example, a particularly damaging hailstorm hit Gannan County, Qiqihar City, China on July 14, 2010, which interrupted the tasseling stage of corn, a critical period for yield formation. Consequently, when a hailstorm occurs, it is necessary and valuable to recognise hail damage and assess the loss as soon as possible, which has become a very vital concern to agricultural production and greatly depends upon crop damage monitoring pre- and post-hailstorm (Jedlovec et al., 2006). Hail-induced corn damage can cause substantial losses for corn growers, so a prompt and accurate method for monitoring and quantifying hail damage to corn can be of great help in the decision making processes of farmers. However, current practices of hail damage detection and assessment have some limitations, especially at a large spatial scale. The traditional damage estimation method mainly depends on labour-intensive field surveys by randomly selecting some sampling points. Then, a statistical model is built to expand to the entire study area. It is obvious that this procedure is time-consuming and is subject to considerable error due to the difficulty in determining the size and spatial location of damaged zones. As a result, monitoring efficiency and evaluation accuracy are inevitably very low. Conversely, remote sensing opens

up an effective and unique avenue for fast and accurate investigations of hail-affected crops. With the advantages of a wide swath, a shorter repetition cycle, multiple sources and multiple resolutions, etc., remote sensing imagery has been widely used in assessing hail damage. In previous studies, different types of aerial and space remotely sensed images have been extensively utilised, including aerial photographs, Landsat thematic mapper/enhanced thematic mapper plus (TM/ETM+), moderate resolution imaging spectroradiometer (MODIS), etc. For instance, Changnon and Barron (1970) evaluated the potential of infrared (IR) colour and standard colour aerial photographs to measure crop hail losses. Gillis et al. (1990) acquired a colour composite transparency of Landsat TM data to map the hail storm damaged areas for an operational salvage harvest in just over two weeks. Parker et al. (2005) investigated severe hailstorm meteorology associated with two elongated swaths of crop damage using time-series MODIS normalised difference vegetation index (NDVI) images. To summarise, when monitoring a hailstorm, remotely sensed data are usually limited by the spatial or temporal resolution of the sensors, so it is impossible to simultaneously derive images with high spatial resolution, a short repetition cycle and wide swath. Furthermore, the adopted methods are too sophisticated to be used for quickly assessing hail damage. As a result, it is difficult to immediately obtain change characteristics and estimate the damage area between pre- and post-hailstorm occurrence. On September 6, 2008, two optical satellites (Huan Jing (HJ)-1 A and B) were successfully launched by China for environmental and disaster monitoring and forecasting. Since then, images with a spatial resolution of 30 m, a wide swath of 360 km and a revisiting period of two days have been received, which have been widely applied in environmental monitoring, land cover/use data updates, land resource investigations, etc. (Chen et al., 2009; Wang et al., 2009; Wang et al., 2010). Nevertheless, no announcements can be found regarding damage detection of hail using HJ-1 imagery according to published reports. Therefore, this study was designed to use a feasible NDVI change detection method to quickly extract the spatial distribution, affected acreage and relative damage levels based on HJ-1 charge-coupled device (CCD) remotely sensed images of China in combination with extensive field survey data.

Description of the study area

Gannan County is located between 122°54′6″ E and 124°28′12″ E, 47°35′7″ N and 48°32′5″ N and administratively belongs to Qiqihar City, Heilongjiang Province, China, about 50 km northwest of the city seat of Qiqihar (Fig. 1a). Currently, there are 4.14 million acres of cultivated land, mainly for soybean, wheat, rice, corn and other grain crops. This area is the transition zone between the Nen River alluvial plain and the Daxingan Forest, which is dominated by the characteristics of a continental monsoon climate. Namely, it is hilly in the west and north, but has flat, open plains in the south and southeast. The terrain altitude of the northwest is higher than that of the southeast, and slowly descends in elevation from 380 to 160 m (Fig. 1b). The average temperature is 2.6°C and the average rainfall is 455 mm. The maximum temperature and rainfall occur from March to October and the minimum temperature and rainfall months occur from November to March (Fig. 1c).

Results

Characterisation of hail-damaged corn

Hailstorms primarily affect yields by defoliating corn and reducing the number of stalks, so the spectral responses of corn are different at different hail-damaged levels (Fig. 4a). Healthy corn illustrates the expected typical vegetation patterns of low reflectance in the visible wavelengths and high reflectance in the near infrared regions. Comparatively, within the visible spectrum, seriously hail-damaged corn shows increased defoliation and results in higher spectral reflectance, while in the near infrared bands, lower radiance is observed. Therefore, the analysis of these spectral curves indicates that there is a positive correlation between the reflectance and damage levels in the visible spectrum, which shows as a negative correlation in the near-infrared spectrum. Similarly, the change trends of Chl and LAI accordingly decrease with an increase in damage severity (Fig. 4b).

Identification of hail-damaged corn

To quickly decide whether a pixel is affected corn, thirty sampling points were used to build a third-order polynomial regression model between Band 4 of the post-hailstorm HJ-1 CCD image and the ΔNDVI image (Fig. 5a). The coefficient of determination (R^2) reached 91.62%. Additionally, twenty sampling points were used to validate the model. As shown in Fig. 5b, R^2 reached 96.31%. Fig. 6a and b represent the NDVI images obtained from the pre- and post-hailstorm HJ-1 CCD scene, showing obvious change from a severe hailstorm in the study area on 14 July 2010. Healthy vegetation and croplands are shown in light grey tones. The areas of the "hail streak" and unaffected fallow fields are in dark grey tones. Fig. 6c shows the ΔNDVI image indicating differences post- and pre-hailstorm. The darker the colour is, the more severe the intensity of the injured corn is. On the ΔNDVI image, the lighter tone indicates an increase in vegetation density between two sampling dates and vice versa. Fig. 6d shows the final extracted corn area which was then merged with the original false-colour composite image (Band 4, Band 3 and Band 2) with healthy vegetation in red tones. The red boxes indicate the affected corn area after the hailstorm. From the identified results, it can be found that the spatial distribution of affected corn was non-uniform due to different hail size and intensity, but it always concentrated in a certain region of the hailstorm. The hail occurrence ran in a northwest to southeast direction and the affected width was greater in the south and north directions than in the east and west.

Specification of hail damage levels

On the basis of extracted affected corn area, a map of damage levels was derived (Fig. 7). It is obvious that the degree of severity gradually descends from the centre to the margin, suggesting that the intensity of hail in certain degree decreased from the centre to the margin of this hailstorm area. Furthermore, it was found that the area of hail-damaged corn mainly concentrated in three towns: Zhongxing, Gannan and Changshan, among which the damage in Zhongxing seemed to be the most severe.

Table 1. Acquired remotely sensed images of HJ-1A/1B CCD and their technical specification for extracting the hail-induced corn area.

Sensor	Acquisition date	Band no.	Spectral range (μm)	Spatial resolution (m)	Repetition cycle (days)	Swath width (km)
HJ-1-B-CCD2 (p453/r56)	2010-07-13	1	0.43~0.52	30	4	360 (single CCD), 700 (dual CCDs)
		2	0.52~0.60	30		
HJ-1-A-CCD2 (p453/r56)	2010-07-19	3	0.63~0.69	30		
		4	0.76~0.90	30		

Table 2. Confusion matrix to evaluate the identification accuracy for different damage levels.

Class	Light	Moderate	Serious	Total
Light	9	2	0	11
Moderate	1	16	2	19
Serious	0	2	18	20
Total	10	20	20	50

Table 3. Acreage statistics and potential yield loss of affected core acreage with different damage levels.

Disaster levels	Estimated damage acreage (ha)	Yield losses (ton)
Light (light impact on corn yield)	2563.29	-
Moderate (mainly distributed along the damage boundary)	3709.62	-
Serious (no grain production)	2302.47	10,840.484*

*The yield of per hectare is the average value of 2005-2009 from the National Bureau of Statistics of China (http://www.stats.gov.cn/)

To evaluate the identification accuracy of hail-induced damage levels, 50 field sample points (10 light points, 20 moderate points and 20 serious points) with different degrees of injury were used to construct a confusion matrix (Table 2). According to the matrix, overall accuracy and κ were obtained. The results show that the overall accuracy and κ were 86% and 0.7826, respectively.

Estimation of hail-damaged acreage and potential yield loss

Based on the multi-temporal HJ-CCD images before and after the hailstorm, the area of hail-damaged corn was estimated (Table 3). There were 8,575.38 ha of corn affected by this hailstorm, and the majority of the corn area was classified as the moderate damage level (3,709.62 ha), followed by the light damage level (2,563.29 ha) and the serious damage level (2,302.47 ha). The reason for this phenomenon is that the crops other than corn were misclassified as corn and bare land was sorted as hail-affected corn because of their similar spectral differences and textural characteristics. Although the affected corn acreage can be determined from the remotely sensed images, the accurate yield loss cannot be accurately predicted. Only the yield loss (10,840.484 tons) of the serious damage level could be evaluated using the average yield data of previous years. The yield losses for the other levels are complex and could be estimated by studying the close relationship between the percentage of defoliation or injuries and the yield in those areas.

Discussion

Hailstorms are a severe and destructive natural disaster which can cause great damage to corn. When a hailstorm occurs, it is urgently required to quickly monitor the spatial distribution and accurately estimate the damaged acreage. However, traditional estimation methods are usually labour-intensive and cannot be used on a large-scale spatial region. Conversely, remote sensing provides a better solution to such a problem with the characteristics of a wide cover, a short repetition cycle, multiple sensors, as well as multi-spectral and multi-temporal resolutions. Therefore, remote sensing is usually used to determine changes following disasters using multi-temporal images pre- and post-disaster. To assess hail damage to corn, it is very feasible to detect these changes using an index sensitive to the change in strong detection of green plant productivity and leaf chlorophyll concentrations. As an important vegetation index, NDVI was first presented in the late 1970s and has become popular in remote sensing since then (Rouse et al., 1974; Roerink et al., 2000; Wardlow et al., 2008). It utilises the correlation between red and infrared radiation by manipulating the digital number values of different bands. Vegetated areas generally have NDVI values greater than zero due to their high near-infrared and low visible reflectance (a characteristic of photosynthesis)(Kriegler et al., 1969). Henebry et al. (2003) used NDVI to highlight abrupt changes in vegetation density by comparing data before and after a storm. In this study, HJ-1 CCD images with a repetition cycle of two days and a spatial resolution of 20 metres, taken pre- and post-hailstorm in Gannan County, were used to assess hail-damaged corn with the assistance of the ΔNDVI image. Owing to the negative effects of the hailstorm, defoliation of corn occurred. This presumably led to yield losses due to decreased ability for effective photosynthesis. It has been identified that the percentage of defoliation using this method is more accurate than an on-site survey 7-10 days after the hailstorm (Erickson et al., 2004). Therefore, remote sensing is useful for identifying and analysing areas affected by hail in immature crops. However, as a cereal crop begins to ripen, remote sensing may not be able to detect the levels of damage effectively because of minimal spectral response variation (Young et al., 2004). Ray (1994) identified that NDVI has the best sensitivity to changes in vegetation cover, except for vegetation cover less than 30%. The analysis of satellite imagery concludes that identifiable spectral variances exist between healthy vegetation and hail-damaged corn; the most pronounced variance occurred in

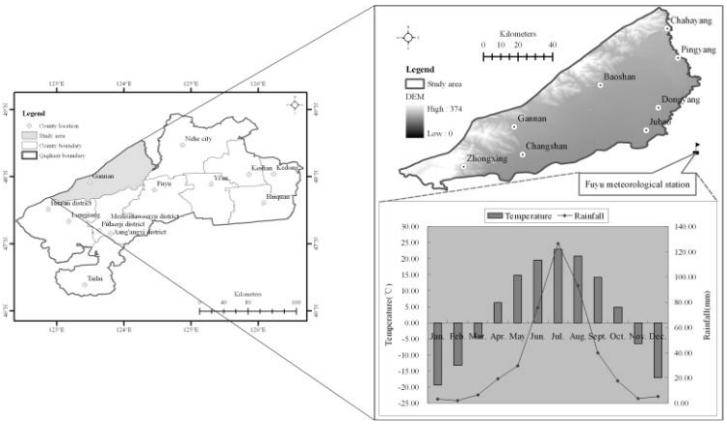

Fig 1. Description of the geographic location (a), topography (b) and climate (c) of Gannan County.

Fig 2. Photographs showing a visual comparison of different damage levels: (a) normal, (b) light, (c) moderate and (d) serious.

the red and near infrared regions of the electromagnetic spectrum. Bands 3 and Band 4 (red and near infrared) can reveal large variations in pixel values. These allow for the assessment and quantification of defoliation from HJ-1 CCD satellite imagery, and form the best band combination for discriminating vegetation defoliation. When detecting hail-induced damage using remotely sensed images, knowing the growth stage is crucial for detection and the following loss assessment. For instance, an assessment of yield loss can help determine whether or not replanting is necessary when a hailstorm occurs earlier in the growing season. If a hailstorm occurs close to the harvesting season, loss assessment can help determine whether or not removal of corn and planting another crop type are necessary in order to minimise economic losses. In this case, the hailstorm occurred at the tasseling stage of corn, so it was possible to identify the affected corn area. Additionally, mixed pixels in agricultural scenes are very common because of current farming practices. For instance, fields of varying stubble, fallow and cropping are commonly found side by side. Fortunately, corn is the dominant crop in Gannan County in this season, while soybean, pumpkin and other crops account for a small percentage of the agricultural land. An exclusion method was first applied to the NDVI data to produce the crop/non-crop map (Lv and Liu, 2010). As shown in Fig. 6, agricultural fields with crops and those in fallow were discernible. Therefore, at the initial stage, unvegetated areas including water, built-up land and bare land were determined. Then, the vegetated land was isolated using an image masking technique. After isolating the healthy vegetation, three relative levels of damage (moderate vegetation, low vegetation and soil) were established, ranging from almost bare soil to moderate vegetation cover. It is assumed that the low vegetation areas would include the hail-damaged area and fallow fields. Compared with the hail-damaged cropland, fallow fields are obvious because most of them have regular rectangular shapes, while the hail damage areas usually have irregular or non-rectangular shapes. Because of constraints on the available data and complex conditions of the study area, the estimated hail-damaged corn acreage was greater than the real conditions. Several reasons contribute to this phenomenon: i. the failure of HJ-1 CCD to differentiate boundaries between corn and other crop types; ii. similarities in the NDVI change trend between corn and some other crop types; iii. beyond the hailstorm, factors such as drought, insects and disease, fertiliser deficiency, etc. can also reduce NDVI values of healthy corn. If more accurate yield loss assessments are needed, the accurate relationship between the defoliation percentage of corn and yield has to be established. Meanwhile, high-resolution temporal and spatial remotely sensed images and adequate ancillary data will also be needed. In addition, according to the features of spatial distribution and the severity degree of hail-damaged corn, it is possible to indirectly predict the characteristics of hailstorms.

Materials and methods

Data source

The satellite and ancillary data used in our study consist of pre- and post-hailstorm HJ-1 CCD satellite images (Table 1), listed by Landsat ETM+ data, canopy spectrum measurements, leaf area index (LAI), chlorophyll content (Chl) and global positioning system (GPS) field positioning sites.

HJ-1 CCD images

Both HJ-1-A and B carry dual CCDs that image four bands with a 30 metre spatial resolution. Therefore, they can shorten the repetition cycle and increase the swath of acquired images. At present, those HJ-1 CCD images acquired from the China Center for Resources and Satellite Data and Applications (CRESDA, http://www.cresda.com.) are systematically processed by geometric and atmospheric corrections. Additionally, the bands of HJ-1 CCD lie in the visual and near-infrared spectrum, so the impact of atmospheric conditions on satellite imagery is greatest at shorter wavelengths where atmospheric scattering is common. As a result, accurate geometric and atmospheric corrections must be performed for reliable analysis. First, atmospheric correction was carried out in the fast line-of-sight atmospheric analysis of spectral hypercubes (FLAASH) module integrated in the ENVI 4.5 (Environment for Visualising Images, Research System Inc.) image processing software. Then, geometric correction was performed in the IMAGINE AutoSync add-on of ERDAS Imagine (Leica Geosystems, Inc.); the registration accuracy was required to be less than 0.5 pixel. This module automatically produces generating thousands of tie points, which can align and orthorectify the HJ-1 CCD images combined with the georeferenced Landsat ETM+ dataset (path/row: 120/026, 120/027, http://glcf.umiacs.umd.edu/). Additionally, image enhancement and haze removal were also performed to improve the interpretation quality of HJ-1 CCD images in ENVI software.

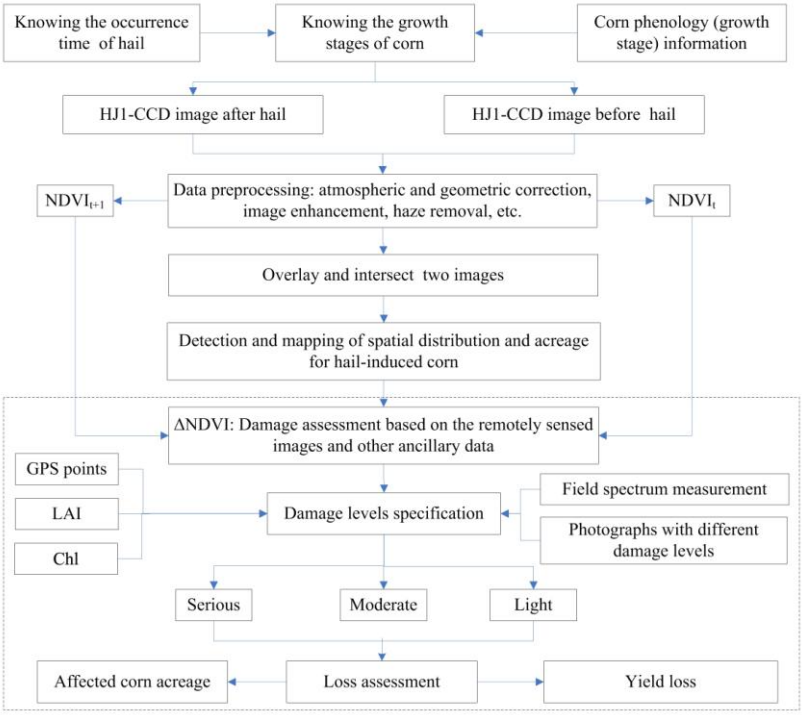

Fig 3. Schematic chart integrating HJ-1 CCD and other ancillary data.

Field survey data

After the occurrence of the hailstorm on July 14, 2010, detailed post-storm field measurements were conducted for deriving ground reference data. After finding hail-damaged corn fields, the damage levels were assessed by agricultural experts and they were positioned using a global positioning system (GPS, Trimble® GeoXH) with an accuracy of less than 1 m. Then, some photographs showed clear visual differences in damaged corn from normal to seriously affected corn (Fig. 2). Meanwhile, canopy spectra were measured using a portable hand-held ASD Field Spectrometer (Analytical Spectral Devices, Inc., Boulder, USA) and the ASD Viewspec Pro 6.0 software and Microsoft Excel were jointly used to perform reflectance conversion. Afterwards, LAI and Chl were also collected using the Sunscan Canopy Analysis System and a SPAD-502 plus chlorophyll meter, respectively.

Overall methodological process

There are in total four steps to determine hail-damaged corn, specify damage levels and estimate yield loss (Fig. 3): assuring the growth stage and selecting available HJ-1 CCD remotely sensed imagery of pre- and post-hailstorm, NDVI difference (Δ NDVI) calculation and damage level specification/loss assessment. First, the time at which the hailstorm occurred should be determined, then the corresponding remotely sensed data and plant growth stage can be identified. In this study, the storm occurred at the tasseling stage of corn and green vegetation dominated most of the corn fields. After the corn was hit by the hailstorm, leaves were broken and vegetation cover accordingly decreased. Therefore, NDVI, which is very sensitive to changes in canopy structure and biomass (Rouse et al., 1974), from HJ-1 CCD satellite images were used to identify the hail-damaged corn area. Considering field samples and photographs of different damage levels, the analysis was performed in terms of damaged acreage, damage levels and potential yield loss.

Calculation of NDVI and ΔNDVI

To better detect changes in vegetation, a ΔNDVI image was generated by simply subtracting the values between the earlier image and the later image. NDVI and ΔNDVI were calculated using the following formulae:

$$\mathrm{NDVI} = (NIR - RED)/(NIR + RED)$$

where *NIR* (0.76-0.90 μm) and *RED* (0.63-0.69 μm) represent the two spectral bands of HJ-1-CCD imagery.

$$\Delta\mathrm{NDVI} = \mathrm{NDVI}_{post} - \mathrm{NDVI}_{pre}$$

where NDVI_{pre} and NDVI_{post} are the NDVI images pre- and post-hailstorm, respectively.

Hail-damaged corn identification

NDVI can represent the growth dynamics of corn and its value increases with the growth of corn and gradually decreases after reaching the maximum at a certain growth stage (Luedeke et al., 1996; Xin et al., 2002). In addition, NDVI is strongly influenced by green plant productivity and leaf chlorophyll concentrations, and can be used to normal-

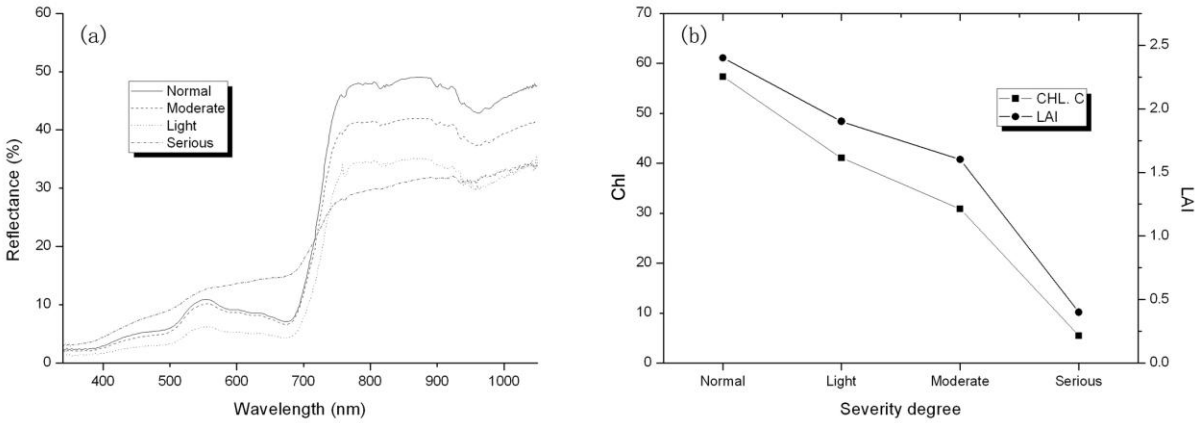

Fig 4. Spectral response curves (a) and change trends of Chl and LAI (b) for different hail damage levels.

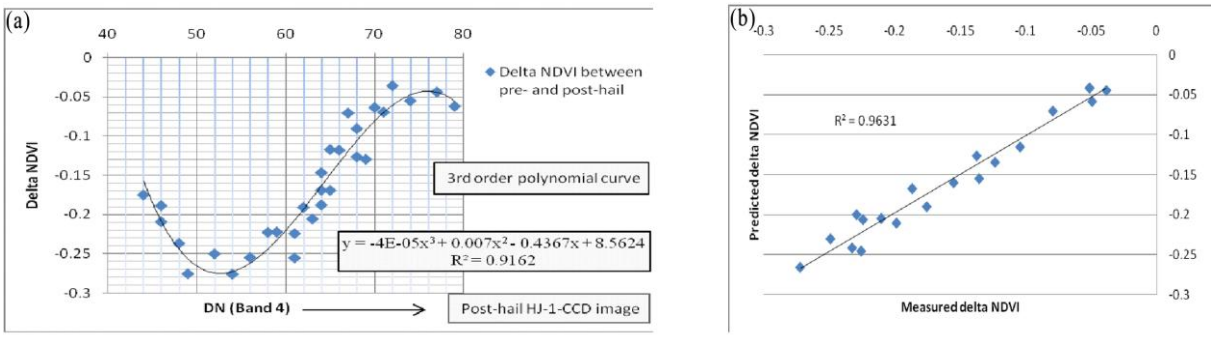

Fig 5. Third-order polynomial (a) and linear regression for accuracy validation (b).

ise the data to a certain degree. Compared with healthy corn, the ΔNDVI of affected corn will show an unexpected change, which can be identified as the affected corn area. Based on the NDVI change detection method, the affected corn area was identified.

Specifying relative severity levels

After identifying the hail-damaged corn area, damage levels were subsequently specified. First of all, the sample sites with GPS coordinates were overlaid onto the ΔNDVI image and the corresponding ΔNDVI values were derived. Subsequently, the means of samples with different damage levels were calculated. Because of the low spectral resolution of HJ-CCD, it is very difficult to derive fine classification in damage levels. Therefore, we chose three relative damage levels in this study: serious, moderate and light depending on the thresholds obtained using the following formulae:

$$\overline{\Delta \mathrm{NDVI}}_{\mathrm{level(j)}} = \Delta \mathrm{NDVI}_1 + \Delta \mathrm{NDVI}_2 + \cdots + \Delta \mathrm{NDVI}_n \big/ n = \sum_{i=1}^{n} \Delta \mathrm{NDVI}_i \big/ n$$

where $\overline{\Delta \mathrm{NDVI}}_{\mathrm{level}(j)}$ is the mean for each level (j) and i (i=1, 2 ,… , n) represents the sample site, of which n is the total number of sample sites for three different damage levels.

$$L_{Serious} = \overline{\Delta NDVI}_{s\ min} \le \Delta NDVI \le \overline{\Delta NDVI}_{s\ max}$$

$$L_{Moderate} = \overline{\Delta NDVI}_{M\ min} \le \Delta NDVI \le \overline{\Delta NDVI}_{M\ max}$$

$$L_{Light} = \overline{\Delta NDVI}_{L\ min} \le \Delta NDVI \le \overline{\Delta NDVI}_{L\ max}$$

where $L_{serious}$, $L_{Moderate}$ and L_{Light} represent the serious, moderate and light damage levels, respectively and $\overline{\Delta NDVI}_{X\ min}$ and $\overline{\Delta NDVI}_{X\ max}$ represent the minimum and maximum values of the three levels, which are derived by calculating the mean of less than or greater than median for sampling sites with three damage levels.

Validation of identification accuracy

To validate the identification results, overall classification accuracy and the Kappa coefficient (κ) were calculated as shown below. κ is another measure of the accuracy of the classification, which is calculated by multiplying the total number of pixels in all the ground truth classes (N) by the sum of the confusion matrix diagonals (x_{kk}), subtracting the sum of the ground truth pixels in a class times the sum of the

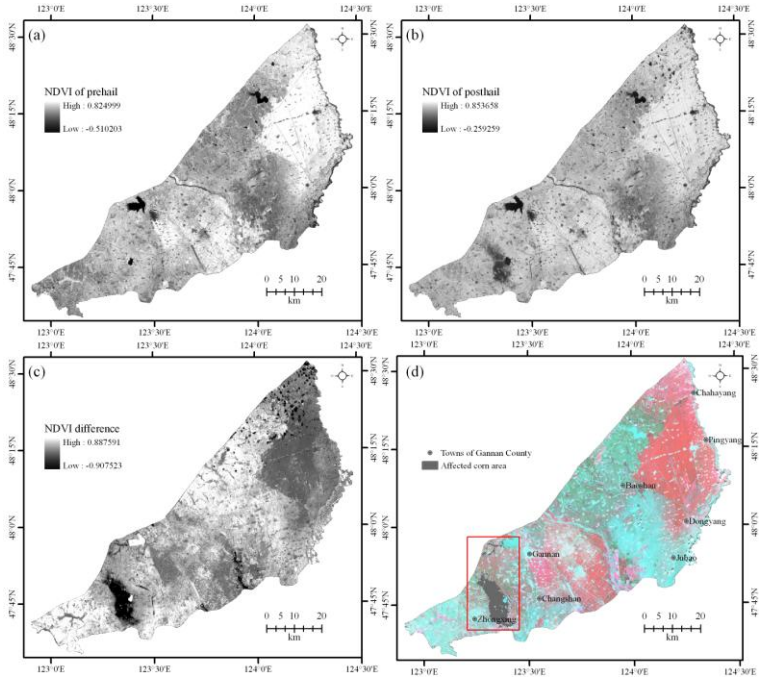

Fig 6. NDVI images (a and b) obtained from the HJ-1-CCD scene, ΔNDVI image (c) and identified affected area (d).

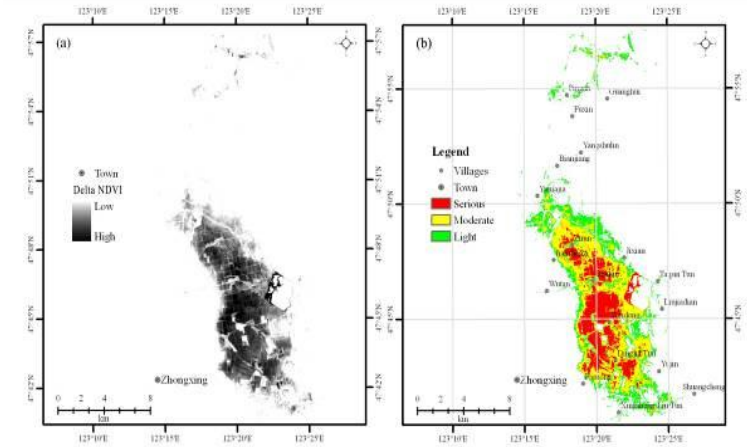

Fig 7. The affected corn area and related severity: (a) NDVI change map of the affected corn area and (b) the final damage level map including three degrees of severity

classified pixels in that class summed over all classes ($x_{k\Sigma}x_{x\Sigma\Sigma}$), and dividing by the total number of pixels squared minus the sum of the ground truth pixels in that class times the sum of the classified pixels in that class summed overall classes.

$$\kappa = \frac{N\sum_{k} x_{kk} - \sum_{k} x_{k\Sigma}x_{x\Sigma k}}{N^2 - \sum_{k} x_{k\Sigma}x_{x\Sigma k}}$$

Conclusion

This study indicates that HJ-1 CCD remotely sensed images can be applied to quickly detect hail-damaged corn acreage and relative levels of hail-damaged corn. With a repetition cycle of two days and a spatial resolution of 30 metres, the ΔNDVI image of HJ-1 CCD pre- and post-hailstorm can be effective to identify hail-damaged corn fields, which is sensitive to corn change. However, due to low spectral resolution, these images are insufficient to derive finer damage levels (serious, moderate and light) from the HJ-1 CCD multi-spectral images, so three relative damage levels were specified according to the thresholds from field sample data. When considering the yield loss caused by a hailstorm, only the serious level corn can be estimated due to complete injury.

Acknowledgements

This research was supported and funded by the National Natural Science Foundation of China (41071276), the Postdoctoral Science Foundation of the Beijing Academy of Agriculture and Forestry Sciences (2011), the Programme of the Ministry of Agriculture (200903010) and Special Funds for Major State Basic Research Project (2007CB714406). The authors are also grateful to Dr. Liu HJ and Mr. Wu HF for their assistance with data collection.

References

Bentley MT, Mote TL, Thebpanya P (2002) Using Landsat to identify thunderstorm damage in agricultural regions. B Am Meteorol Soc 83:363–37

Changnon SA, Barron NA (1970) Quantification of crop-hail losses by aerial photography. J Appl Meteorol 10:86–96

Chen SR, Sun H, Zhang BJ (2009) Application research and implementation of drought monitoring by HJ-1A/1B satellites. Spacecraft Engineering 18:138–141 (in Chinese)

Erickson BJ, Johannsen CJ, Vorst JJ, Biehl LL (2004) Using remote sensing to assess stand loss and defoliation in maize. Photogramm Eng Rem S 70:717–722

Gillis MD, Pick RD, Leckie DG (1990) Satellite imagery assists in the assessment of hail damage for salvage harvest. Forest Chron 66:463–468

Golden JH, Snow JT (1991) Mitigation against extreme windstorms. Rev Geophys 29:477–504.

Henebry GM, Ratcliffe IC (2003) Occurrence and persistence of hailstreaks in the vegetated land surface. Paper presented at the proceedings of the 83rd annual meeting of the American Meteorological Society, Long Beach, CA, 9-13 February 2003

Jedlovec GJ, Nair U, Haines SL (2006) Detection of storm damage tracks with EOS data. Weather Forecast 21:249–267

Kriegler FJ, Malila WA, Nalepka RF, Richardson W (1969) Preprocessing transformations and their effects on multispectral recognition. Paper presented at the proceedings of the sixth international symposium on remote sensing of the environment, University of Michigan, Ann Arbor, MI, 13-16 October 1969

Luedeke MKB, Ramge PH, Kohlmaier GH (1996) The use of satellite NDVI data for the validation of global vegetation phenology models: application to the Frankfurt biosphere model. Ecol Model 91:255–270

Lv TT, Liu C (2010) Study on extraction of crop information using time-series MODIS data in the Chao Phraya Basin of Thailand. Adv Space Res 45: 775–784

Mirza MMQ (2003) Climate change and extreme weather events: can developing countries adapt? Clim Policy 3:233–248

Parker MD, Ratcliffe IC, Henebry GM (2005) The July 2003 Dakota hailswaths: Creation, characteristics, and possible impacts. Mon Weather Rev 133:1241–1260

Peters AJ, Griffin SC, Vina A (2000) Use of remotely sensed data for assessing crop hail damage. Photogramm Eng Rem S 66:1349–1355

Ray TW (1994) A FAQ on vegetation in remote sensing. California Institute of Technology, Pasadena, California, USA

Roerink GJ, Menenti M (2000) Reconstructing cloudfree NDVI composites using Fourier analysis of time series. Int J Remote Sens 21:1911–1917

Rouse JW, Haas RH, Schell JA, Deering DW (1974) Monitoring vegetation systems in the Great Plains with ERTS. Paper presented at the proceedings of the third earth resources technology satellite-1 symposium, Goddard Space Flight Center, Washington, D.C., 10-14 December 1973

Tai FJ, Yuan ZL, Wu XL, Zhao PF, Hu XL, Wang W (2011) Identification of membrane proteins in maize leaves, altered in expression under drought stress through polyethylene glycol treatment. Plant Omics 4(5):250-256

Wang Q, Wu C Q, Li Q (2010) Environment Satellite 1 and its application in environmental monitoring. Journal of Remote Sensing 14:102–112 (in Chinese)

Wang ZT, Li Q, Tao JH., Li SS, Wang Q, Chen LF (2009) Monitoring of aerosol optical depth over land surface using CCD camera on HJ-1 satellite. China Environmental Science 29:902–907 (in Chinese)

Wardlow BD, Egbert SL (2008) Large-area crop mapping using time-series MODIS 250 m NDVI data: An assessment for the U.S. Central Great Plains. Remote Sens Environ 112:1096–1116

Xin JF, Yu ZR, van Leeuwen L, Driessen PM (2002) Mapping crop key phenological stages in the North China Plain using NOAA time series images. Int J Appl Earth Obs 4:109–117

Young FR., Chandler O, Apan A (2004) Crop hail damage: insurance loss assessment using remote sensing. Paper presented at the proceedings of annual conference of the Remote Sensing and Photogrammetry Society, Aberdeen, UK, 7-10 September 2004